analytical chemistry

pubs.acs.org/ac Article

Monoclonal Antibody-Based Biosensor for Point-of-Care Detection of Type III Secretion System Expressing Pathogens

Yaron Hillman, Jenia Gershberg, Dan Lustiger, Dan Even, Dor Braverman, Yael Dror, Idan Ashur, Sefi Vernick, Neta Sal-Man,* and Yariv Wine*

Cite This: https://dx.doi.org/10.1021/acs.analchem.0c03621 Read Online

ACCESS | Metrics & More | Article Recommendations | Supporting Information

ABSTRACT: It is predicted that the antibiotic resistance crisis will result in an annual death rate of 10 million people by the year 2050. To grapple with the challenges of the impending crisis, there is an urgent need for novel and rapid diagnostic tools. In this study, we developed a novel monoclonal antibody—named mAb-EspB-B7—that targets the EspB protein, a component within the bacterial type 3 secretion system (T3SS), which is mainly expressed in Gram-negative pathogens and is essential for bacterial infectivity. We found that mAb-EspB-B7 has high affinity and specificity toward recombinant and native EspB proteins; is stable over a range of pH levels, temperatures, and salt concentrations; and retains its functionality in human serum. We identified the epitope for mAb-EspB-B7 and validated it by competitive enzyme-linked immunosorbent assay (ELISA). Since this epitope is conserved across several T3SS-harboring pathogens, mAb-EspB-B7 holds great potential for development as an active component in precise and rapid diagnostic tools that can differentiate between commensal and pathogenic bacterial strains. To this end, we integrated the well-characterized monoclonal antibody into an electrochemical biosensor and demonstrated its high specificity and sensitivity capabilities in detecting pathogenic bacterial T3SS-associated antigens as well as intact bacteria. We foresee that in the near future it will be possible to design and develop a point-of-care biosensor with multiplexing capabilities for the detection of a panel of pathogenic bacteria.

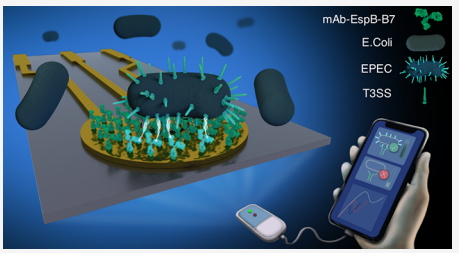

INTRODUCTION

The emergence of multiple-drug resistant (MDR) bacterial strains stems largely from the extensive, and sometimes inappropriate, usage of antibiotics in the community and in agriculture, as this misuse has exerted a strong selective pressure on bacteria to develop resistance mechanisms against various antibiotics.[1,2] In turn, the implications of the increasing numbers of MDR bacterial infections in the clinic, in the community, and in agriculture are constituting a growing global public health concern.[3] MDR bacterial infections are harder to treat and are associated with higher medical costs than antibiotic-sensitive infections, and, perhaps more importantly, there is a significant risk that MDR mechanisms will be spread to other bacterial strains.[4] A parallel public health concern is that the development and approval of new antibiotics has not kept pace with the rising rates of morbidity and mortality due to bacterial infections, giving rise to a predicted annual death rate of 10 million people by 2050 due to resistance to antimicrobials.[5]

Pivotal to the efficiency of controlling antibiotic resistance is the ability to provide rapid and accurate surveillance and diagnosis,[6] as is embodied in the WHO One Health concept for addressing the MDR crisis.[7] In this regard, the major disadvantages of currently available laboratory-based diagnostics for the detection of bacterial infections are long processing times, low sensitivity and specificity, and/or the need for specialized equipment that is expensive and requires highly trained personnel.[8−10] There is, thus, an imperative need for more rapid, cost-effective, and sensitive assays that can identify infective agents at the point-of-care (POC), without the requirement for multistep processing.

A particularly promising means for providing such diagnosis lies in monoclonal antibodies (mAbs) targeted against pathogen-specific antigens. mAbs were previously demonstrated as diagnostic agents for the detection of harmful bacteria.[11−14] In keeping with this line of thought, recent advances in the discovery, engineering, production, and clinical development of mAbs indicate their potential in the design of rapid diagnostics.

A major need for rapid diagnosis includes strains of Gram-negative bacterial pathogens, such as *Escherichia coli*, and species of *Salmonella*, *Shigella*, *Yersinia*, and *Pseudomonas*, which cause serious diseases, ranging from lethal diarrhea to sepsis, leading to millions of deaths annually.[10,15,16] An essential component common to these bacterial pathogens is

Received: August 25, 2020
Accepted: December 3, 2020

termed the type 3 secretion system (T3SS). The T3SS is a syringe-like protein complex, which is responsible for injecting virulence factors from the bacterial cytoplasm directly into the human host cell.[17] This T3SS complex is essential for bacterial virulence, as the injected proteins (effectors) manipulate key intracellular host pathways (e.g., cell cycle, immune response, cytoskeletal organization, metabolic processes, and intracellular trafficking) that ultimately promote bacterial replication and transmission.[18,19]

In the current study, we focused on the development of a T3SS-specific mAb and its use in a bioelectronic diagnostic device for the detection of enteropathogenic *E. coli* (EPEC), the causative agent of infantile diarrhea.[10] EPEC contains a T3SS, which is absent from the nonpathogenic strains of *E. coli*. The EPEC T3SS comprises more than 20 proteins, three of which—EspA, EspB, and EspD—are highly exposed to the extracellular environment. EspA forms a long filamentous structure that bridges between the bacterial and host cells, and EspB and EspD together form a translocator pore complex that facilitates the passage of effectors across the host plasma membrane. Of these three proteins, we chose to develop a mAb (mAb-EspB-B7) with high affinity and specificity to the T3SS protein, EspB.

Our rational for pinpointing EspB derived from the fact that EspB is getting exposed to the extracellular environment following EPEC entrance to the digestive system and in response to thermal and chemical signals.[20,21] Based on the number of T3SS complexes expressed on each bacteria and the predicted number of EspB subunits found in each T3SS complex, we estimate that there are approximately 100 EspB molecules per each bacterial cell.[22−24] Here, we report the development and characterization of mAb-EspB-B7 and further demonstrate its potential as a bio-recognition element in a reliable and easy-to-use electrochemical biosensor. The mAb-EspB-B7 demonstrated high specificity and affinity toward EspB, binding capacity to soluble EspB and in the context of whole bacteria, and high stability under a variety of conditions. These characteristics make mAb-EspB-B7 an excellent candidate to serve as an integral component of a mAb-based biosensor. Indeed, a biosensor based on mAb-EspB-B7 demonstrated excellent performance in recognizing both soluble EspB and in the context of the whole bacteria. Such a biosensor can be used to monitor bacterial infections in the community and provide rapid results at the POC.

EXPERIMENTAL SECTION

The full description of the experimental for bacterial strains, expression and purification of recombinant EspB, phage panning, mAb-EspB-B7 expression and purification, enzyme-linked immunosorbent assay (ELISA), surface plasmon resonance (SPR), flow cytometry, and epitope mapping is given in the Supporting Information.

***In Vitro* Type 3 Secretion Assay.** *In vitro* T3SS assay was carried out as described previously for EPEC[25] and *Salmonella*.[26] Detailed assay protocol can be found in the Supporting Information.

Immunoblotting. Samples were subject to immunoblotting as described previously.[27] For specific details, refer to the Supporting Information.

Co-elution of EspB and EspD-^{35}His by Nickel Affinity Chromatography. Co-elution assays were performed as previously described.[27,28] Detailed co-elution protocol can be found in the Supporting Information.

Effector Translocation Activity. Translocation assays were performed as previously described.[29] For further details, see the Supporting Information.

Electrochemical Biosensor Fabrication. Electrochemical biochips were fabricated and biofunctionalized as previously reported.[30−32] Further details are provided in the Supporting Information.

Biosensor Measurements. The experimental description for biosensor measurements is provided in the Supporting Information.

RESULTS

Binding Affinity and Specificity of mAb-EspB-B7 to EspB. To evaluate the binding affinity of mAb-EspB-B7 to EspB, we performed ELISA (Figure 1A) and SPR (Figure 1B)

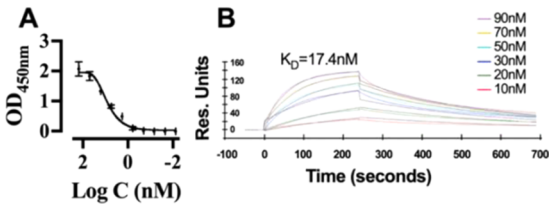

Figure 1. mAb-EspB-B7 binds EspB with high affinity. (A) mAb-EspB-B7 binding affinity to purified EspB was evaluated by ELISA. A 96-well plate coated with EspB was incubated with serially diluted mAb-EspB-B7. mAb-EspB-B7 binding was determined using anti-human IgG HRP-conjugated antibody. The error bars represent ± standard deviation (SD). (B) SPR sensorgrams of mAb-EspB-B7 binding to an EspB-coated chip. mAb-EspB-B7 was added at various concentrations between 10 and 90 nM. Sensorgrams were fitted to the steady-state model.

binding assays. We found that mAb-EspB-B7 binds EspB with high affinity, with a K_D value of 17.4 nM. To determine whether mAb-EspB-B7 binds specifically to EspB under native conditions, we examined the binding of mAb-EspB-B7 to WT EPEC, Δ*escN* (a mutant lacking a functional T3SS), Δ*espB* (a mutant that does not express and secrete EspB), and Δ*espB* + EspB-His (an *espB* null strain that overexpresses plasmid-encoded EspB-His). The different strains grown under T3SS-inducing conditions were separated into bacterial pellets and supernatants, which were then analyzed by sodium dodecyl sulfate polyacrylamide gel electrophoresis (SDS-PAGE) and western blot using mAb-EspB-B7 in the detection phase. In agreement with a previous study, we detected significant secretion of EspB into the bacterial supernatant of WT EPEC, but not into the supernatants of the Δ*escN* or Δ*espB* mutants (Figure 2A).[27] Moreover, we observed that overexpression of EspB (Δ*espB* + EspB-His) resulted in a higher expression of the protein within the bacteria (pellet) as well as a higher secretion into the extracellular medium (Figure 2A).

mAb-EspB-B7 Binding to EspB in the Assembled T3SS. To examine whether mAb-EspB-B7 can bind to the native protein in the assembled T3SS, we used flow cytometry. For this purpose, the bacterial strains grown under T3SS-inducing conditions were incubated first with mAb-EspB-B7 and then with a secondary antibody conjugated to a fluorophore. As expected, mAb-EspB-B7 binding was detected in WT EPEC and in the Δ*espB* strain overexpressing EspB, whereas no or minimal binding was detected in the Δ*escN* and Δ*espB* mutant strains (Figure 2B).

https://dx.doi.org/10.1021/acs.analchem.0c03621
Anal. Chem. XXXX, XXX, XXX−XXX

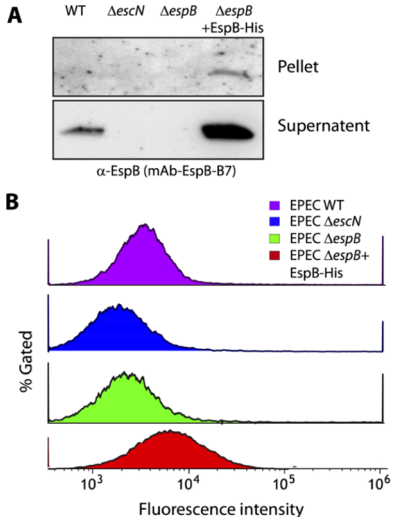

Figure 2. mAb-EspB-B7 binds to recombinant and native EspB. (A) EPEC wild type (WT), Δ*escN*, Δ*espB*, and Δ*espB* expressing EspB-His strains were grown under T3SS-inducing conditions for 6 h. The bacterial pellets and supernatants were separated and analyzed using SDS-PAGE and western blotting with mAb-EspB-B7. EspB expression within the bacteria (pellet) was observed only for the Δ*espB* + EspB-His strain, while EspB secretion (supernatant) was observed for both WT EPEC and the complemented Δ*espB* + EspB-His strain. (B) EPEC WT, Δ*escN*, Δ*espB*, and Δ*espB* + EspB-His bacteria were grown under T3SS-inducing conditions for 3 h. Thereafter, 1×10^7 bacteria were incubated with mAb-EspB-B7, washed, and stained with Alexa Fluor 488 goat anti-human IgG antibody. Flow cytometry analysis was performed on a Gallios instrument (Beckman coulter).

Stability of mAb-EspB-B7 Binding under Various Physiochemical Conditions. We evaluated the ability of mAb-EspB-B7 to bind EspB under various conditions by ELISA. We found that incubation of mAb-EspB-B7 in human serum did not compromise the ability of the antibody to bind EspB compared to its binding in a 3% milk solution (Figure 3A). Examination of mAb-EspB-B7 binding under different pH conditions demonstrated that the binding was essentially not altered under a wide range of pH values (5.6−7.4), with the exception of pH 4.6, at which (as expected) there was a reduction in binding capacity (Figure 3B). Interestingly, testing

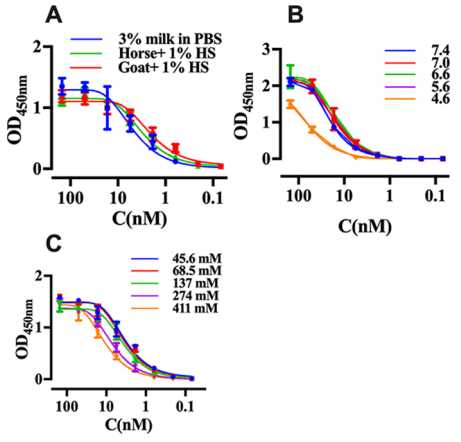

Figure 3. mAb-EspB-B7 binding to EspB under various conditions. mAb-EspB-B7 binding to EspB was evaluated by ELISA (A) in different media, (B) under various pH conditions, and (C) at different NaCl concentrations. The error bars represent ± SD.

mAb-EspB-B7 across a wide range of NaCl concentrations demonstrated that only increased salt concentrations (>250 mM) affected the binding capacity of the antibody (Figure 3C). Finally, to assess the thermal stability of mAb-EspB-B7, we determined its melting temperature, both alone and in complex with purified EspB, using nanoDSF. The melting temperatures of 75.4 and 82°C for mAb-EspB-B7 alone and in complex with EspB, respectively (Figure S1), indicated high mAb stability.

Noninterference of mAb-EspB-B7 with the EspB−EspD Interaction. The EspB protein is found in a complex with another T3SS protein, called EspD, within the assembled T3SS.[33] To confirm that the mAb-EspB-B7 epitope is exposed following EspB−EspD interaction, we evaluated the ability of EspB to co-elute with EspD in the absence or presence of mAb-EspB-B7 (100 or 200 nM). We observed that the presence of mAb-EspB-B7 did not affect the co-elution of EspB with EspD (Figure 4), suggesting that mAb-EspB-B7 does not

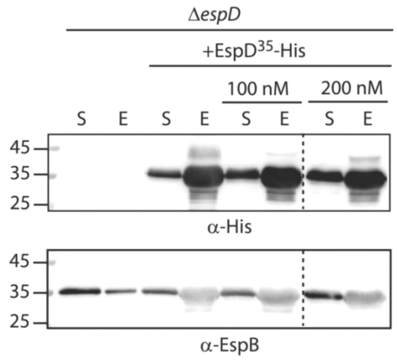

Figure 4. mAb-EspB-B7 does not interfere with the EspB−EspD interaction. Supernatants of EPEC Δ*espD* expressing EspD-^{35}His were purified using Ni-NTA beads. EPEC Δ*espD* strain without the pEspD-^{35}His expression vector was used as a negative control. Samples of supernatants (S) and elution (E) fractions were loaded on SDS-PAGE and analyzed by western blotting with mouse anti-His and anti-EspB antibodies (to avoid detection of the human EspB antibody). Analysis of the supernatants confirmed EspB and EspD secretion into the extracellular medium. The co-elution of EspB with EspD-^{35}His was not affected by the absence or presence (100 and 200 nM) of mAb-EspB-B7. Low EspB nonspecific binding to the Ni-NTA beads was detected (in the absence of EspD-^{35}His).

interfere with the EspB−EspD interaction. Low nonspecific binding of EspB to the Ni-NTA beads was observed in the negative control (a sample that did not express EspD-^{35}His).

mAb-EspB-B7 Epitope Mapping. To identify the exact epitope of mAb-EspB-B7 within the EspB protein, we designed a peptide array of 78 cyclic peptides that covers the full sequence of EspB (321 residues long). Each peptide was 15 residues long, with an overlap of 11 residues between the peptides. Recombinant EspB (full-length) served as a positive control, while bovine serum albumin (BSA) served as a negative control. Incubation of mAb-EspB-B7 with the peptide array revealed that mAb-EspB-B7 bound mostly to two cyclic peptides within the array, namely, to peptides #49 (positions 193−207) and #50 (positions 197−211), which have the sequences TSAQKASQVAEEAAD and KASQVAEEAA-DAAQE of the EspB protein, respectively (Figure 5A). To confirm that this epitope is indeed recognized by mAb-EspB-B7, we synthesized the following peptides: peptide #49; peptide #50; a peptide that comprises the combined sequences

https://dx.doi.org/10.1021/acs.analchem.0c03621
Anal. Chem. XXXX, XXX, XXX−XXX

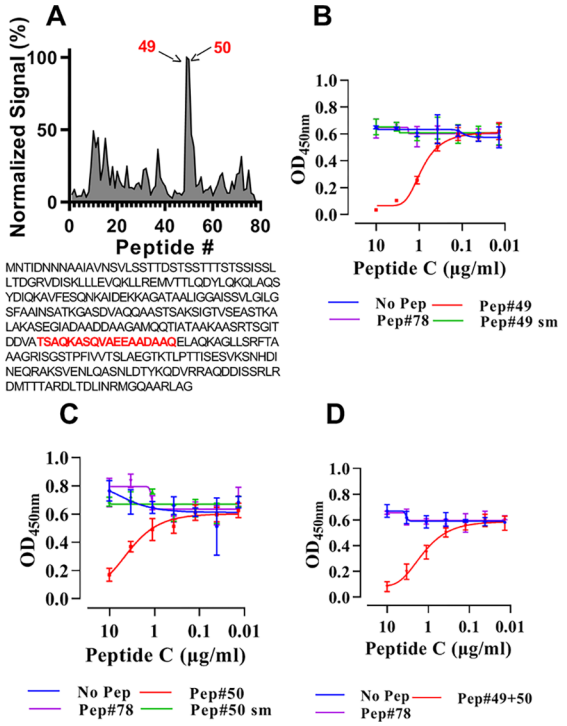

Figure 5. mAb-EspB-B7 epitope mapping. (A) An EspB pepstar peptide array of 78 cyclic peptides (15-residue-long peptides with an 11-residue overlap) was examined for mAb-EspB-B7 binding. Image analysis was carried out with Genepix Pro 6.0 analysis software (Molecular Devices) to detect antibody binding; fluorescence signals were normalized showing their relative intensities. The putative binding site of mAb-EspB-B7 along the EspB protein is marked in red. The arrows indicate the signals obtained from peptides #49 and #50, which displayed the highest signal intensities. (B–D) mAb-EspB-B7 binding to EspB following preincubation with peptide #49 and peptide #49 scrambled (B), peptide #50 and peptide #50 scrambled (C), or peptide #49 + 50 (D) was evaluated by competitive ELISA and detected using anti-human IgG HRP-conjugated antibody. Peptide #78 was used as a negative control. The error bars represent ± SD.

of peptides #49 and #50 (TSAQKASQVAEEAADAAQE); peptide #78, which was not detected by the mAb-EspB-B7 and was therefore suitable as a negative control; and two peptides with scrambled sequences of peptides #49 and #50. Competitive ELISA between full-length EspB and the cyclic peptides revealed that preincubation of peptides #49, #50, or #49 + #50 (1 μg/mL) with mAb-EspB-B7 completely abolished the ability of the antibody to bind full-length EspB (Figure 5B–D). To determine whether the competitive effect is derived directly from the binding of mAb-EspB-B7 to the peptides, we assessed the ability of mAb-EspB-B7 to recognize and bind these peptides. We observed that mAb-EspB-B7 can bind peptides #49, #50, and the combined peptide (#49 + #50), while no binding was detected for the scrambled peptides or for peptide #78 (Figure S2A–C). These results confirm that the main mAb-EspB-B7 epitope is the KASQVAEEAAD sequence of the EspB protein (peptide sequences are presented in Figure S2D).

mAb-EspB-B7 Specificity toward EPEC EspB Homologs. To assess the specificity of mAb-EspB-B7 toward EspB homologs in other bacterial pathogens and its potential to be used for detection of bacteria related to other infectious diseases, bacterial cultures grown under T3SS-inducing conditions were centrifuged, and supernatants and pellets were analyzed by SDS-PAGE and western blotting using mAb-EspB-B7. The following WT bacteria and T3SS-mutant strains were cultured: EPEC; enterohemorrhagic *E. coli* (EHEC), which causes a more severe disease than EPEC in humans; *Citrobacter rodentium*, an EPEC-related mouse pathogen; and *Salmonella enterica serovar Typhimurium*, which utilizes two T3SSs for virulence. The strongest signal was observed for the WT EPEC supernatant; a significant, but less strong, a signal was also detected for *C. rodentium*; and an even less strong signal was observed for EHEC (Figure 6). However, no signals

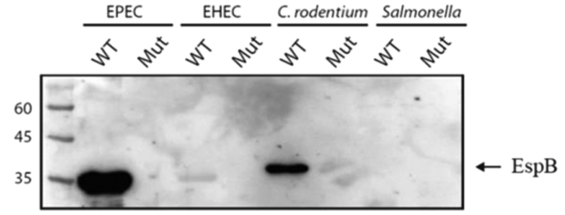

Figure 6. mAb-EspB-B7 binds EspB homologs in other T3SS-expressing bacteria. Wild-type and mutant EPEC, EHEC, *C. rodentium*, and *Salmonella* were grown under T3SS-inducing conditions. EPEC, EHEC, and *C. rodentium* mutant strains contain a deletion in the *escN* gene, while *Salmonella* contains a deletion in the *invA* gene, which results in nonfunctional T3SSs in these mutants. The bacterial cultures were centrifuged, and the supernatants were collected, normalized, and analyzed by SDS-PAGE and western blotting using mAb-EspB-B7.

were detected in the supernatants of *Salmonella* or any of the T3SS-mutant strains. Sequence alignment of EPEC and *C. rodentium* EspB proteins revealed high conservation between the proteins and full conservation of the mAb-EspB-B7 epitope sequence. Sequence alignment between EPEC and EHEC EspB proteins revealed 80% similarity at the mAb-EspB-B7 epitope region (Figure S3).

Effect of mAb-EspB-B7 on Bacterial–Host Cell Interaction. To examine the ability of mAb-EspB-B7 to directly interfere with the bacterial infection of host cells, we examined the translocation activity of WT EPEC in the presence or absence of mAb-EspB-B7. For that purpose, we infected HeLa cells with EPEC strains (WT and Δ*escN*) and examined the cleavage pattern of JNK, a host protein that is cleaved by a translocated EPEC effector known as NleD (Figure S4A).[29] WT EPEC caused extensive degradation of JNK, relative to the uninfected sample and the samples infected with the Δ*escN* mutant strain (Figure S4B). We found that HeLa cells infected by WT EPEC in the presence of a high concentration of mAb-EspB-B7 (400 nM) showed translocation activity similar to that of WT EPEC infection with no addition of antibody. These results suggest that while mAb-EspB-B7 was capable of binding EspB with high affinity and specificity, this binding did not interfere with the protein function and did not inhibit the T3SS translocation activity in an *ex vivo* model.

Development of mAb-EspB-B7-Based Biosensor and Its Application in Detecting Purified EspB Protein and EspB-Presenting Bacteria. The potential of the developed mAb-EspB-B7 in diagnostic applications may be exploited by integrating it with an electrochemical biosensor. In particular, impedimetric immunosensors show great promise in rapidly detecting low concentrations of target antigens within a highly simplified testing setup.[34,35] We sought to demonstrate this

https://dx.doi.org/10.1021/acs.analchem.0c03621
Anal. Chem. XXXX, XXX, XXX–XXX

potential by constructing a miniature electrochemical biochip functionalized with mAb-EspB-B7, as illustrated in Figure 7A. The impedance measurements yielded Nyquist plots that were fitted to an equivalent circuit from which charge transfer resistance (R_{ct}) values were obtained (see Supporting methods pages S4–S5 for further description). We recorded electrochemical impedance spectra (EIS) for the electrodes before and after antibody immobilization, and these were compared with measurements taken after a 10 min incubation of purified EspB protein at varying concentrations. Using the Nyquist plot (Figure 7B), we observed the effect of mAb-EspB-B7 immobilization on the R_{ct}. In a bare electrode, the resistance to charge transfer is small and impedance is dominated by mass transfer (diffusion of the electroactive species), the so-called Warburg impedance, which is evident in low frequencies.[36] The Warburg impedance is considerably decreased following mAb immobilization as mass transfer is no longer a significant factor. Instead, the contribution of R_{ct} to the impedance is now largely dominant, as an insulating layer of biomolecules is attached to the surface. Following a brief incubation of 250 μg/mL purified EspB solution, we observed a significant increase in R_{ct}, which is directly correlated with the bound antigen concentration further adding to the resistive component of the impedance. We found that the addition of purified EspB protein affects the R_{ct} in a dose-dependent manner, enabling the distinction between different concentrations (Figure 7C). In addition, incubation of a nonspecific antigen (microcystin toxin) showed no effect on the measured R_{ct}. Similarly, no effect was observed from purified EspB protein directly incubated on a bare electrode (Figure 7C), indicating that the change in R_{ct} reflects the specific binding of EspB to the mAB-EspB-B7 antibody. The relative change in R_{ct} exhibits an exponential dependence on concentration, as seen in Figure 7D.

To examine the applicability of mAb-EspB-B7-based electrochemical biosensing in detecting whole bacteria harboring T3SS (and present EspB), we grew WT EPEC and Δ*espB* mutant strains under T3SS-inducing conditions and incubated bacterial samples on the biochip. As shown in Figure 7E, higher R_{ct} values were consistently recorded for EPEC WT (mean R_{ct} change = 1.22 ± 0.09) compared to the Δ*espB* mutant strain (mean R_{ct} change = 0.86 ± 0.12). The minimal binding of the Δ*espB* strain was likely due to nonspecific adsorption. It should be noted that following centrifugation and lack of T3SS-inducing conditions, shedding of the complex is likely to occur, consistent with our western blot analysis shown in Figure 2. Nevertheless, the obtained signals were shown to be significantly higher (36% ± 15) in response to EPEC WT compared to the Δ*espB* strain (p = 0.03). Overall, these results demonstrated the potential of our biosensor to detect EspB, both in its secreted form and an integral component of the assembled T3SS complex in the context of whole bacteria.

DISCUSSION

In recent years, advances in mAb discovery and production have ushered in the development of pathogen-specific mAb's to be used either per se as antibacterial drugs or to be integrated into various diagnostic platforms for the detection of specific pathogens. In the latter regard, the high affinity and specificity of mAbs are characteristics that can be exploited in diagnostic tools giving reduced false-positive/-negative results. Such tools could provide rapid and accurate identification of

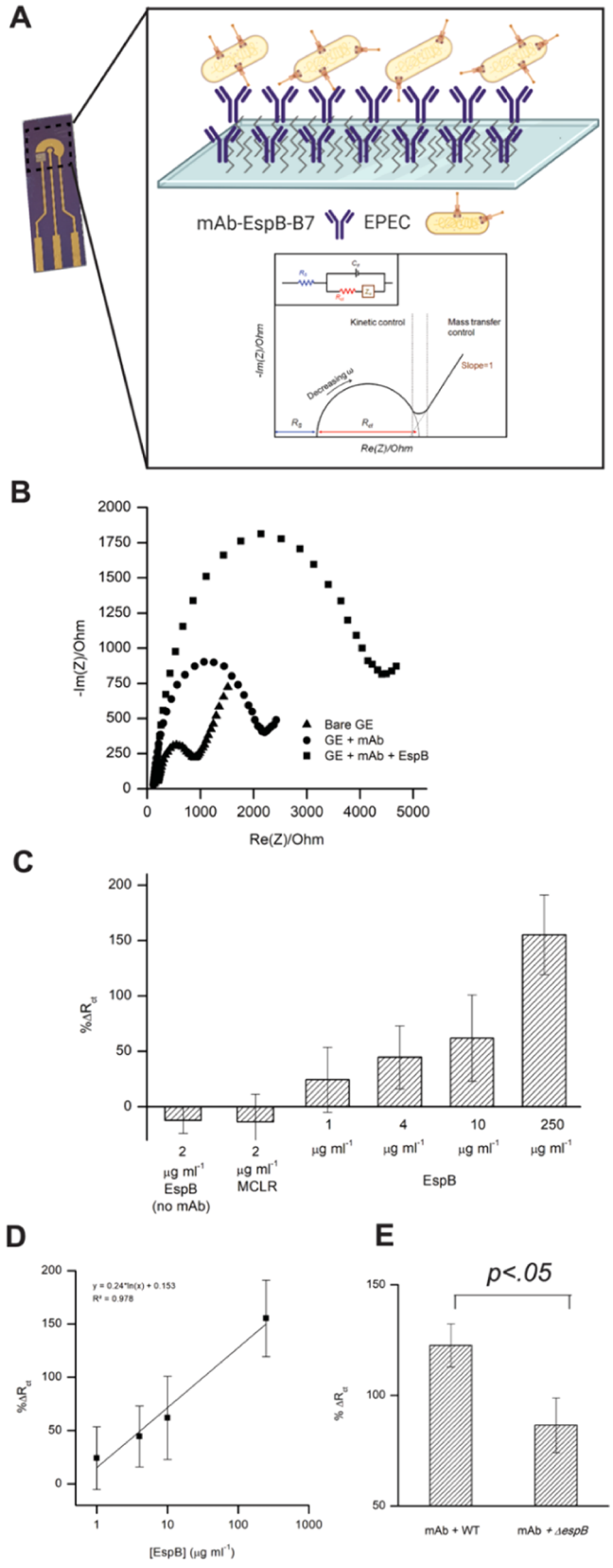

Figure 7. mAb-EspB-B7-based impedimetric biosensor. (A) EIS-based detection of whole EPEC cells is illustrated. Electrochemical chips (with a working electrode radius of 0.6 mm) are fabricated in-house using microelectronic fabrication technologies and are subsequently modified with a thiolated mAb-EspB-B7 using thiol-gold chemistry. The immobilization of mAb-EspB-B7 and capture of

https://dx.doi.org/10.1021/acs.analchem.0c03621
Anal. Chem. XXXX, XXX, XXX−XXX

Figure 7. continued

antigen affect the impedance of the underlying electrode. An EIS measurement thus allows for the interrogation of the electrochemical system and separation of the individual components that affect the circuit. The generated Nyquist plot is fitted to an equivalent circuit from which the different resistance values are extracted (inset). (B) The obtained Nyquist plots from measurements of a bare gold electrode (bare GE), electrode after the immobilization of mAb-EspB-B7 (GE+mAb), and mAb-EspB-B7-coated electrode after incubation with 250 μg/mL purified EspB protein (GE+mAb+EspB). (C) Relative R_{ct} values of purified EspB protein (1, 4, 10, and 250 μg/mL) demonstrating a dose-dependent increase in R_{ct}. No binding was observed with an unrelated purified protein microcystin-LR (2 μg/mL). In addition, incubation of purified EspB protein (2 μg/mL) on a bare electrode (without mAB-EspB-B7) showed no binding of EspB, further supporting the specificity of the biosensor. Relative R_{ct} values are the means of the R_{ct} ratios (before and after antigen capture) calculated from three to six measurements. The error bars represent ± SD. (D) Change in R_{ct} is exponentially dependent on EspB concentration. (E) Specific binding of WT EPEC cells is indicated, resulting in a larger contribution to R_{ct} compared with the Δ*espB* null strain. The percent change in R_{ct} ratios measured for EPEC WT and Δ*espB* was calculated and averaged from 20 repeats (five measurements each containing four samples) for each strain. The mean of the averaged ratios and the standard error of the mean were calculated.

bacterial agents at POC, thus supporting better clinical management of patients and preventing the transmission of infectious diseases in the community.

Here, we describe an mAb raised against EspB, an essential component within the T3SS that is crucial for the infectivity of numerous Gram-negative bacteria, including EPEC. Our results demonstrate that mAb-EspB-B7 binds EspB with nM affinity and high specificity. As commercial monoclonal antibodies against bacterial species, targeted mostly against common bacterial antigen such as the flagella or the bacterial Lipopolysaccharides (LPS), have been reported to have micromolar affinities,[37,38] the mAb-EspB-B7 holds greater potential to allow efficient detection of bacterial pathogens due to its nM affinity.

The antibody binding to its EspB target was stable over a wide range of pH values, excluding acidic pH values, and across various salt concentrations. A reduced binding capacity was detected only under high salt concentrations (>250 mM), suggesting that the antibody−antigen binding interface is governed by electrostatic interactions. This idea is supported by the observation that the identified EspB epitope contains nearly 50% of charged amino acids, which might be involved in the antibody−antigen binding. mAb-EspB-B7 demonstrated a relatively high melting temperature, which was moderately elevated when the antibody was complexed with its antigen. This result suggests that EspB binding has a stabilizing effect on the antibody, as was previously reported for anti-ricin neutralizing antibody.[39] Furthermore, the melting temperature profile of mAb-EspB-B7 showed three distinct events that probably correspond to the melting order of the C_H2 region, followed by the Fab and C_H3, as reported previously.[40] This melting profile indicates that mAb-EspB-B7 would be suitable for applications that require relatively high thermal stability.

Epitope mapping using our specially designed cyclic-peptide array revealed that mAb-EspB-B7 binds mostly to a specific amino acid sequence located at positions 193−210 along the EspB sequence. In a previous study, it was shown that this region was not important for EspB−EspD interactions,[28] a fact that was further corroborated by our observation that mAb-EspB-B7 does not disrupt the interaction between the two proteins. Moreover, the observation that mAb-EspB-B7 binds EspB as a component of the fully assembled T3SS complex supports the notion that the epitope of EspB is exposed and not buried within the EspB−EspD interface. It is noteworthy that the peptide array results also identified an additional region, corresponding to peptides #9−12, that demonstrated mAb-EspB-B7 binding. This finding could perhaps suggest that the epitope recognized by mAb-EspB-B7 is conformational rather than linear. As the main epitope sequence (positions 193−210) is fully conserved in EPEC and *C. rodentium*, the lower similarity along this second region might provide an explanation for the reduced western blot signal that we observed for *C. rodentium* EspB (Figure 6A). In addition, while we observed mAb-EspB-B7 binding to a protein in the supernatants of WT EHEC and *C. rodentium*, no binding was detected in the *Salmonella* supernatant. This result is in agreement with the presence of the epitope in EHEC and *C. rodentium* but not in *Salmonella* (Figure S3).

The ability of mAb-EspB-B7 to recognize and bind *C. rodentium* EspB is highly important, as it provides the scientific grounds for the use of the mAb-EspB-B7 antibody as a diagnosis tool of mice infection model. In addition, while mAb-EspB-B7 did not demonstrate a reduction of bacterial infectivity in the *ex vivo* system, we posit that examining it in a mouse model will provide a more comprehensive picture that will include the effect of the antibody in promoting certain activities of the immune system against bacteria, such as opsonization and phagocytic clearance. These activities may prevent the spread of the bacterial infection within the host body and induce a humoral response with serological memory that will shorten the infection duration, promote recovery, and provide cellular and serological memory.

Another key aspect of mAb-EspB-B7 is its ability to bind both the secreted forms of EspB and EspB as a component of the assembled T3SS complex within the bacterial cell. This finding provides further support for its potential as a diagnostic agent capable of detecting bacterial infections directly in clinical samples in a short time with high accuracy, as previously reported.[41,42]

Demonstrating the diagnostic potential of mAb-EspB-B7 in electrochemical biosensing is particularly interesting. Here, we developed a biochip, functionalized it with the specific mAb-EspB-B7, and applied a label-free, EIS-based detection of EspB or, alternatively, EspB-presenting bacteria by simply incubating the sample for several minutes. Our direct approach to electrode functionalization is advantageous compared to well-established self-assembled monolayer (SAM) generation methods since it involves a straightforward preparation and avoids a complete electrode passivation often achieved with SAM. We have shown that despite obvious limitations related to nonspecific adsorption and sample inhomogeneity, the biosensor provides a concentration-dependent signal that can be fit to an exponential function yielding a calibration curve. Nonlinear calibration curves have been previously reported in impedimetric biosensors.[43,44] In addition, we observed that the biosensor differentiates between T3SS-containing and T3SS-lacking bacteria, thus providing a simple tool to detect pathogenic bacteria.

https://dx.doi.org/10.1021/acs.analchem.0c03621
Anal. Chem. XXXX, XXX, XXX−XXX

CONCLUSIONS

In this study, we characterized the mAb-EspB-B7 that binds with high affinity and selectivity to a T3SS-exposed protein and provided a proof of concept that this antibody can be integrated into a miniaturized electrochemical biosensor that can identify T3SS-containing bacteria. Future work with this antibody should focus on its development for an antibacterial drug and as part of a high-throughput diagnostic device, such as a portable standalone antibody-based biosensor.

ASSOCIATED CONTENT

Supporting Information

The Supporting Information is available free of charge at https://pubs.acs.org/doi/10.1021/acs.analchem.0c03621.

Expression and purification of recombinant EspB, enzyme-linked immunosorbent assay (ELISA), surface plasmon resonance (SPR), in vitro type 3 secretion assay, immunoblotting, flow cytometry, co-elution of EspB and EspD35-His by nickel affinity chromatography, epitope mapping using peptide array, effector translocation activity, electrochemical biosensor fabrication, biosensor measurements, nano-differential scanning fluorimetry (nanoDSF); mAb-EspB-B7 is thermally stable (Figure S1); mAb-EspB-B7 binding to EspB peptides (Figure S2); and mAb-EspB-B7 does not inhibit EPEC translocation activity into HeLa cells (Figure S3) (PDF)

AUTHOR INFORMATION

Corresponding Authors

Neta Sal-Man − *Department of Microbiology, Immunology and Genetics, Faculty of Health Sciences, Ben-Gurion University of the Negev, Beer Sheva 8410501, Israel;* orcid.org/0000-0002-1109-479X; Email: salmanne@bgu.ac.il

Yariv Wine − *The Shmunis School of Biomedicine and Cancer Research, George S. Wise Faculty of Life Sciences, Green building, Tel-Aviv University, Tel Aviv 6997801, Israel;* orcid.org/0000-0001-5767-9059; Email: yarivwine@tauex.tau.ac.il

Authors

Yaron Hillman − *The Shmunis School of Biomedicine and Cancer Research, George S. Wise Faculty of Life Sciences, Green building, Tel-Aviv University, Tel Aviv 6997801, Israel*

Jenia Gershberg − *Department of Microbiology, Immunology and Genetics, Faculty of Health Sciences, Ben-Gurion University of the Negev, Beer Sheva 8410501, Israel*

Dan Lustiger − *The Shmunis School of Biomedicine and Cancer Research, George S. Wise Faculty of Life Sciences, Green building, Tel-Aviv University, Tel Aviv 6997801, Israel*

Dan Even − *The Shmunis School of Biomedicine and Cancer Research, George S. Wise Faculty of Life Sciences, Green building, Tel-Aviv University, Tel Aviv 6997801, Israel*

Dor Braverman − *Department of Microbiology, Immunology and Genetics, Faculty of Health Sciences, Ben-Gurion University of the Negev, Beer Sheva 8410501, Israel*

Yael Dror − *The Shmunis School of Biomedicine and Cancer Research, George S. Wise Faculty of Life Sciences, Green building, Tel-Aviv University, Tel Aviv 6997801, Israel*

Idan Ashur − *Institute of Agricultural Engineering, Agricultural Research Organization, Rishon Lezion 5025001, Israel*

Sefi Vernick − *Institute of Agricultural Engineering, Agricultural Research Organization, Rishon Lezion 5025001, Israel*

Complete contact information is available at: https://pubs.acs.org/10.1021/acs.analchem.0c03621

Author Contributions

Y.H., J.G., and D.L. contributed equally. Y.W., N.S., and S.V. designed the experiments and wrote the manuscript. Y.H., J.G., D.L., D.E., D.B., Y.D., and I.A. performed the experiments. Y.H., J.G., and I.A. analyzed the data.

Funding

This research was supported by the Israel Ministry of Economy—Kamin Grant Numbers: 61970 (Y.W.) and 61971 (N.S.), The Israel Ministry of Science and Technology Grant Number 3−16841 (N.S. and Y.W.), and Israel Scientific Foundation grant number 988/19 (N.S.).

Notes

The authors declare no competing financial interest.

ACKNOWLEDGMENTS

The authors thank Salam Bashir (Tel Aviv University) for his kind assistance with the data analysis of the peptide array, Dikla Hiya and Dr. Yael Pazy Benhar (Technion Center for Structural Biology) for their generous assistance with operating the nanoDSF instrument, and Dr. Aharon Rabinkov (Weizmann Institute Core Facilities) for his assistance with operating the SPR instrument. They also thank Prof. Itai Benhar (Tel Aviv University) for kindly providing a human synthetic phage displaying scFv library for phage panning and Yael Diesendruck for assisting with the panning procedure.

REFERENCES

(1) Laxminarayan, R.; Duse, A.; Wattal, C.; Zaidi, A. K.; Wertheim, H. F.; Sumpradit, N.; Vlieghe, E.; Hara, G. L.; Gould, I. M.; Goossens, H.; Greko, C.; So, A. D.; Bigdeli, M.; Tomson, G.; Woodhouse, W.; Ombaka, E.; Peralta, A. Q.; Qamar, F. N.; Mir, F.; Kariuki, S.; Bhutta, Z. A.; Coates, A.; Bergstrom, R.; Wright, G. D.; Brown, E. D.; Cars, O. *Lancet Infect. Dis.* **2013**, *13*, 1057−1098.

(2) Laxminarayan, R.; Heymann, D. L. *BMJ* **2012**, *344*, No. e1567.

(3) Ventola, C. L. *Pharm. Ther.* **2015**, *40*, 277−283.

(4) Jiang, X.; Ellabaan, M. M. H.; Charusanti, P.; Munck, C.; Blin, K.; Tong, Y.; Weber, T.; Sommer, M. O. A.; Lee, S. Y. *Nat. Commun.* **2017**, *8*, No. 15784.

(5) O'Neill, J. *Review on Antibacterial Resistance: Tackling Drug-Resistant Infections Globally*; UK Government and the Wellcome Trust, 2016.

(6) Levin, B. R.; Baquero, F.; Johnsen, P. J. *Curr. Opin. Microbiol.* **2014**, *19*, 83−89.

(7) Hernando-Amado, S.; Coque, T. M.; Baquero, F.; Martinez, J. L. *Nat. Microbiol.* **2019**, *4*, 1432−1442.

(8) Fournier, P. E.; Drancourt, M.; Colson, P.; Rolain, J. M.; La Scola, B.; Raoult, D. *Nat. Rev. Microbiol.* **2013**, *11*, 574−585.

(9) Burnham, C.-A. D.; Carroll, K. C. *Clin. Microbiol. Rev.* **2013**, *26*, 604−630.

(10) Croxen, M. A.; Law, R. J.; Scholz, R.; Keeney, K. M.; Wlodarska, M.; Finlay, B. B. *Clin. Microbiol. Rev.* **2013**, *26*, 822−880.

(11) Guttikonda, S.; Tang, X. L.; Yang, B. M.; Armstrong, G. D.; Suresh, M. R. *J. Immunol. Methods* **2007**, *327*, 1−9.

(12) Yang, X.; He, Z.; Zhang, G.; Lu, J.; Zhang, H.; Ren, H.; Tian, Y.; Yang, H.; Chen, C.; Li, L.; Fu, Y.; Allain, J. P.; Li, C.; Wang, W. *Front. Cell Infect. Microbiol.* **2020**, *10*, 145.
(13) Ghasemi, R.; Mirahmadi-Zare, S. Z.; Nasr-Esfahani, M. H.; Allafchian, A.; Behmanesh, M. *Anal. Bioanal. Chem.* **2019**, *411*, 6733−6743.
(14) Jampasa, S.; Lae-Ngee, P.; Patarakul, K.; Ngamrojanavanich, N.; Chailapakul, O.; Rodthongkum, N. *Biosens. Bioelectron.* **2019**, *142*, No. 111539.
(15) Dekker, J. P.; Frank, K. M. *Clin. Lab. Med.* **2015**, *35*, 225−246.
(16) Khalil, I. A.; Troeger, C.; Blacker, B. F.; Rao, P. C.; Brown, A.; Atherly, D. E.; Brewer, T. G.; Engmann, C. M.; Houpt, E. R.; Kang, G.; Kotloff, K. L.; Levine, M. M.; Luby, S. P.; MacLennan, C. A.; Pan, W. K.; Pavlinac, P. B.; Platts-Mills, J. A.; Qadri, F.; Riddle, M. S.; Ryan, E. T.; Shoultz, D. A.; Steele, A. D.; Walson, J. L.; Sanders, J. W.; Mokdad, A. H.; Murray, C. J. L.; Hay, S. I.; Reiner, R. C., Jr. *Lancet Infect. Dis.* **2018**, *18*, 1229−1240.
(17) Kaper, J. B.; Nataro, J. P.; Mobley, H. L. *Nat. Rev. Microbiol.* **2004**, *2*, 123−140.
(18) Cornelis, G. R. *Nat. Rev. Microbiol.* **2006**, *4*, 811−825.
(19) Bhavsar, A. P.; Guttman, J. A.; Finlay, B. B. *Nature* **2007**, *449*, 827−834.
(20) Mellies, J. L.; Barron, A. M.; Carmona, A. M. *Infect. Immun.* **2007**, *75*, 4199−4210.
(21) Kenny, B.; Abe, A.; Stein, M.; Finlay, B. B. *Infect. Immun.* **1997**, *65*, 2606−2612.
(22) Daniell, S. J.; Takahashi, N.; Wilson, R.; Friedberg, D.; Rosenshine, I.; Booy, F. P.; Shaw, R. K.; Knutton, S.; Frankel, G.; Aizawa, S. *Cell Microbiol.* **2001**, *3*, 865−871.
(23) Wilson, R. K.; Shaw, R. K.; Daniell, S.; Knutton, S.; Frankel, G. *Cell Microbiol.* **2001**, *3*, 753−762.
(24) Romano, F. B.; Tang, Y.; Rossi, K. C.; Monopoli, K. R.; Ross, J. L.; Heuck, A. P. *J. Biol. Chem.* **2016**, *291*, 6304−6315.
(25) Tseytin, I.; Madar, A.; Mitrovic, B.; Deng, W.; Finlay, B. B.; Sal-Man, N. *mSphere* **2018**, 3.
(26) Kujat Choy, S. L.; Boyle, E. C.; Gal-Mor, O.; Goode, D. L.; Valdez, Y.; Vallance, B. A.; Finlay, B. B. *Infect. Immun.* **2004**, *72*, 5115−5125.
(27) Luo, W.; Donnenberg, M. S. *Infect. Immun.* **2006**, *74*, 810−820.
(28) Luo, W.; Donnenberg, M. S. x. *J. Bacteriol.* **2011**, *193*, 2972−2980.
(29) Baruch, K.; Gur-Arie, L.; Nadler, C.; Koby, S.; Yerushalmi, G.; Ben-Neriah, Y.; Yogev, O.; Shaulian, E.; Guttman, C.; Zarivach, R.; Rosenshine, I. *EMBO J.* **2011**, *30*, 221−231.
(30) Porat-Ophir, C.; Belkin, A.; Vernick, S.; Dergachev, V.; Freynd, G.; Katsnelson, M.; Shacham-Diamand, Y. *ECS Electrochem. Lett.* **2013**, *2*, G8−G10.
(31) Vernick, S.; Niv, Y.; Vilkin, A.; Freeman, A.; Shacham-Diamand, Y. *Gastroenterology* **2012**, *142*, S345.
(32) Vernick, S.; Freeman, A.; Rishpon, J.; Niv, Y.; Vilkin, A.; Shacham-Diamand, Y. *J. Electrochem. Soc.* **2011**, *158*, P1−P4.
(33) Luo, W.; Donnenberg, M. S. *J. Bacteriol.* **2011**, *193*, 2972−2980.
(34) Randviir, E. P.; Banks, C. E. *Anal. Methods* **2013**, *5*, 1098−1115.
(35) Siddiqui, S.; Dai, Z.; Stavis, C. J.; Zeng, H.; Moldovan, N.; Hamers, R. J.; Carlisle, J. A.; Arumugam, P. U. *Biosens. Bioelectron.* **2012**, *35*, 284−290.
(36) Lasia, A. Impedance of the Faradaic Reactions in the Presence of Mass Transfer. In *Electrochemical Impedance Spectroscopy and its Applications*; Springer New York: New York, NY, 2014; pp 85−125.
(37) Hearty, S.; Leonard, P.; Quinn, J.; O'Kennedy, R. *J. Microbiol. Methods* **2006**, *66*, 294−312.
(38) Hurley, J. C. *Toxins* **2013**, *5*, 2589−2620.
(39) Legler, P. M.; Compton, J. R.; Hale, M. L.; Anderson, G. P.; Olson, M. A.; Millard, C. B.; Goldman, E. R. *MAbs* **2017**, *9*, 43−57.
(40) Vermeer, A. W.; Norde, W. *Biophys. J.* **2000**, *78*, 394−404.
(41) Barreiros dos Santos, M.; Agusil, J. P.; Prieto-Simon, B.; Sporer, C.; Teixeira, V.; Samitier, J. *Biosens. Bioelectron.* **2013**, *45*, 174−180.
(42) Joung, C. K.; Kim, H. N.; Lim, M. C.; Jeon, T. J.; Kim, H. Y.; Kim, Y. R. *Biosens. Bioelectron.* **2013**, *44*, 210−215.
(43) Lu, L.; Chee, G.; Yamada, K.; Jun, S. *Biosens. Bioelectron.* **2013**, *42*, 492−495.
(44) Barreiros dos Santos, M.; Sporer, C.; Sanvicens, N.; Pascual, N.; Errachid, A.; Martinez, E.; Marco, M. P.; Teixeira, V.; Samiter, J. *Procedia Chem.* **2009**, *1*, 1291−1294.

https://dx.doi.org/10.1021/acs.analchem.0c03621
Anal. Chem. XXXX, XXX, XXX−XXX